Proceedings of the Korean Nuclear Autumn Meeting
Yongpyong, Korea, October 2002

An Effective Monitoring of Calandria Reactor Surface using A Low-cost Thermal Infrared Camera and A CCD Camera.

Jai Wan Cho, Chang Hoi Kim, Young Soo Choi, Yong Chil Seo, and Seung Ho Kim

Korea Atomic Energy Research Institute
P.O.Box 105, Yusong, Daejon, Korea 305-600

Abstract

In this paper an approach to enhance inspection performances for calandria reactor area of Wolsung nuclear power plant through the technique of superimposing thermal infrared image into real CCD image is introduced. Thermal infrared imaging is a highly promising technology for condition monitoring and predictive maintenance of electronic, electrical and mechanical elements in nuclear power plants. We have developed a visible CCD/thermal infrared inspection head module for these monitoring purposes, which we use in conjunction with the PULNiX TM-7CN CCD camera and a FLIR THV510 thermal infrared camera. In the occurrence of thermal abnormalities on observation points and areas of calandria reactor area, unusual hot image taken from thermal infrared camera is mapped upon real CCD image. We used a circular pattern of pressure tubes placed on the front surface of the calandria reactor as plate for camera calibration needed to match the FOV between thermal camera and CCD camera. The performance of the technique has been evaluated in the experiment carried out at Wolsung nuclear power plant in the overhaul period. The results show that localizations of thermal abnormalities on calandria reactor surface can be estimated accurately.

1. Introduction

Thermal infrared imaging techniques are now used in monitoring the conditions of many kinds of engines, electrical and mechanical elements, and processes in a variety of industrial plants.[1][2] The aerospace industry uses these techniques for locating defects in thin aluminum aircraft skins.[3][4] These techniques have also been shown to be well suited for the detection of delaminations and subsurface impact damage in many advanced composite materials.[5][6] These techniques have even been used to detect structural defects in large bridge concrete decks.[7] Lawrence Livermore National Laboratory (LLNL) uses dual-band infrared thermal imaging to identify and remove non-thermal IR reflectance backgrounds from foreign material on the roadway.[8] DBIR thermal imaging allows precise temperature measurement to reliably locate bridge deck delaminations and remove wavelength-dependent emissivity variations due to foreign material on the roadway. Defects such as cracks, inclusions, voids, or delaminations conduct heat at a rate different from that of the defect-free material. This causes gray level gradients to develop at the surface of defect material that can be detected by a thermal infrared camera. Mobile Robot is being considered for number of surveillance, inspection, predictive maintenance, early warning, and potentially maintenance applications of nuclear power plant. A thermal infrared imaging system is needed to confirm and localize a fault in calandria reactor area of CANDU-type nuclear power plant. The fault could be a blocked or leaking feeder pipe, or damaged insulation in that area. Many industrial plants use thermal infrared imaging system carried on a mobile robot for this purpose. Although trouble-shooting images taken from thermal infrared camera cannot be considered as maintenance, even less as predictive maintenance. For this purpose, KAERI is developing a mobile robot KAEROT/m2 for CANDU-type nuclear power plant applications, which can be adapted for defense applications such as NBC detection.[9] This KAEROT/m2 consists of moving mechanism and sensing mechanism. We have developed a visible CCD/thermal infrared inspection head module for KAEROT/m2 mobile robot as the sensing mechanism, which we use in conjunction with the PULNiX TM-7CN CCD camera and a FLIR THV510 thermal infrared camera. The THV510 is commercially available low-cost thermal infrared camera. However, the low-cost thermal infrared camera suffers from poor spatial resolution compared to commercial CCD cameras. This paper describes an approach to enhance inspection performances for calandria reactor area of Wolsung nuclear power plant through the technique of superimposing thermal infrared image into real CCD image. In the occurrence of thermal abnormalities on observation points and areas of calandria reactor area, unusual hot image taken from thermal infrared camera is mapped upon real CCD image.

2. Inspection Head

The inspection head module for KAEROT/m2 mobile robot consists of a visible CCD camera and a thermal infrared camera. The thermal infrared camera is AGEMA THV510, which is commercially available low-cost one. The inspection head module can be schematically seen in Figure 1. The THV510 thermal infrared camera and the CCD camera are placed in parallel. The narrower the horizontal distance between the thermal infrared camera and the CCD camera is, the larger the shared FOV in the horizontal direction. The distance between the thermal infrared and CCD camera in the horizontal direction is 153mm. The lens diameter of a THV510 is 70mm. The Y-Axis offset is set at 20mm to match the center of the TM-7CN CCD camera lens, 52mm, and the one of THV510. The 6X motorized zoom lens, 11.5~69mm, is selected as the TM-7CN CCD camera lens to capture the wide dynamic range imagery for the enhanced inspection purpose. The technical specifications of the inspection head are shown in Table 1.[10] THV510 thermal infrared camera use 1-dimensional array sensor, which have formats, 160 X 1 cells, composed of InSb FPA device. The two-dimensional infrared image is obtained by scanning mechanism of infrared optics. The array sensor placed in vertical direction, are scanned in horizontally, in 512 steps. One field image, 512 X 160 pixels, is created by this horizontal scan mechanism. And the array sensor is moved one step in vertical direction. That means vertical IFOV and interlaced scan, 1.3 mrad, as showed in Table 1. And then, the above horizontal scan mechanism is done once more to create full image, 512 X 320 pixels, NTSC

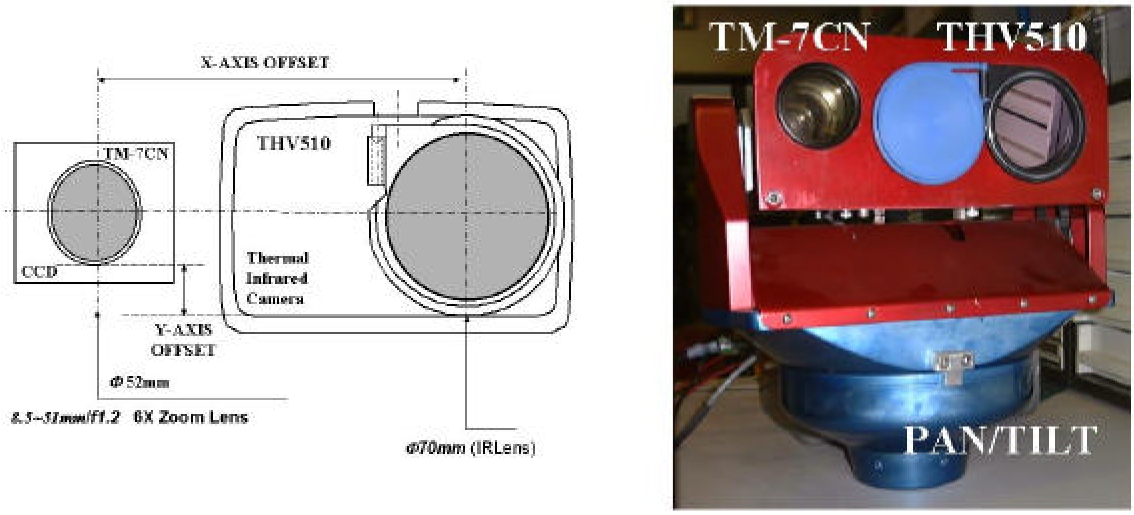

Fig. 1. Inspection head for KAEROT/m2 mobile robot

Table 1. Inspection head specification

Parameters	Technical Specifications	
	THV510	TM-7CN
FOV	18.3 X 9.15° [H X V]	7.2 ~ 41.2° [H]
Spectrum	3 ~ 5 um	0.4 ~ 0.7 um
Detector	160 Elements InSb FPA	1/2” IT CCD
IFOV	1.0 X 1.3 mrad	6.45 X 4.84 mm
Field rate	15Hz	60Hz
Focus	0.7m ~	11.5 ~ 69mm
Cell Size		0.84 X 0.98um[H X V]
Sensitivity	0.1°C @ 30°C	
Image	512 X 320	768 X 494 [H X V]
Dimension	260 X 140 X 320 mm [W X H X D]	
Weight	Approx. 5 kg	

video signal. This infrared image obtained from electro-optical scanning method have disadvantage of jitter compared to expensive thermal camera using 2-dimensional array sensor, 320 X 240 pixel format device. The jitter is generated by electrical step pulse signal to drive the motor of infrared scan optics.

3. Calibration of THV510 and TM-7CN

The FOV of THV510, 18.3° X 9.15° in horizontal and vertical direction, and the one of TM-7CN attached 6X zoom lens, 7.2 ~ 41.2° in horizontal direction, are different as shown in table 1. The FOV of thermal infrared camera is fixed, and one of CCD is variable as attached lens type. In order to accurately superimpose thermal image into visible CCD image, it is necessary to match the FOV of the THV510 and TM-7CN. Figure 2 illustrates the relationship between the thermal infrared camera and CCD camera attached zoom lens.

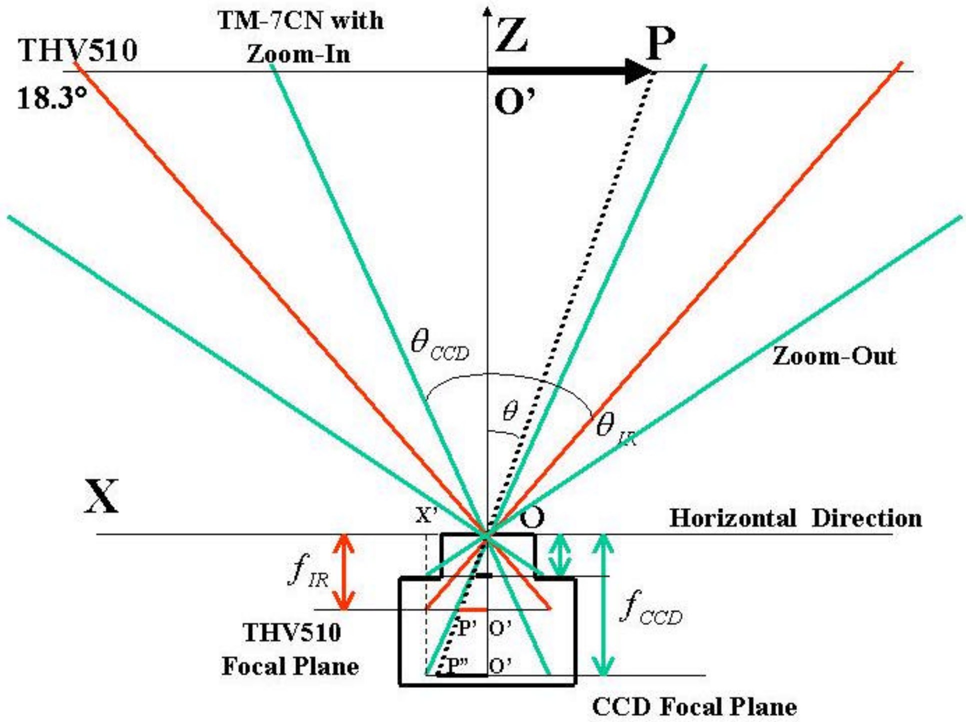

Figure 2. FOV of THV510 and CCD camera.

In this paper, we assume that there is no lens distortion in zoom lens of CCD camera. The focal length of THV510 f_{IR}, is to be estimated using the FOV angle θ_{IR}, assumed that the sensor dimensions of both cameras are the same in horizontal or vertical directions. The focal length of THV510 is shortened, wide FOV, or lengthened, narrow FOV, as the one of CCD lens is changed from zoom-out to zoom-in status in the above assumptions. It means that the imaging size of THV510 is focused in the CCD image frame at the rate, f_{CCD}/f_{IR}. The size of object, $\overline{O'P}$, is focused to $\overline{O'P'}$, in the THV510 image frame, and focused to $\overline{O'P''}$, in the CCD image frame. The FOV calibration relations between TM-7CN and THV510 are given by following formula.

$$\overline{O'P'} = f_{IR}\tan\theta \qquad (1)$$

$$\overline{O'P''} = f_{CCD}\tan\theta \qquad (2)$$

$$f_{IR}\tan\theta_{IR} = f_{CCD}\tan\theta_{CCD} \qquad (3)$$

$$\overline{O'P'} = \overline{O'P''}\tan\theta_{CCD}/\tan\theta_{IR} \qquad (4)$$

In formula (4), θ_{CCD}, θ_{IR} represents FOV angles of TM-7CN and THV510 in horizontal direction. The FOV angle of TM-7CN, θ_{CCD}, is widened or narrowed as the zoom status. The imaging size, $\overline{O'P'}$, of THV510 superimposed into the CCD image frame is enlarged or reduced as the rate, $\tan\theta_{CCD}/\tan\theta_{IR}$, is greater than 1 or less than 1. In formula (4), the THV510 FOV angle, θ_{IR}, is fixed at 18.3° in horizontal direction, and known variable. The TM-7CN FOV angle, θ_{CCD}, unknown variable, is needed for matching of CCD image and infrared image. Generally, in order to obtain lens parameters, intrinsic and extrinsic, camera calibration method is used. Camera calibration in the context of 3-D machine vision is the process of determining the internal camera geometric, intrinsic parameters, and the 3-D position and orientation of the camera frame relative to a world coordinates system, extrinsic parameters. [11] In this paper, we used Tsai' s proposed calibration algorithm. The procedure for camera calibration is to use calibration chart, shown in Figure 3.

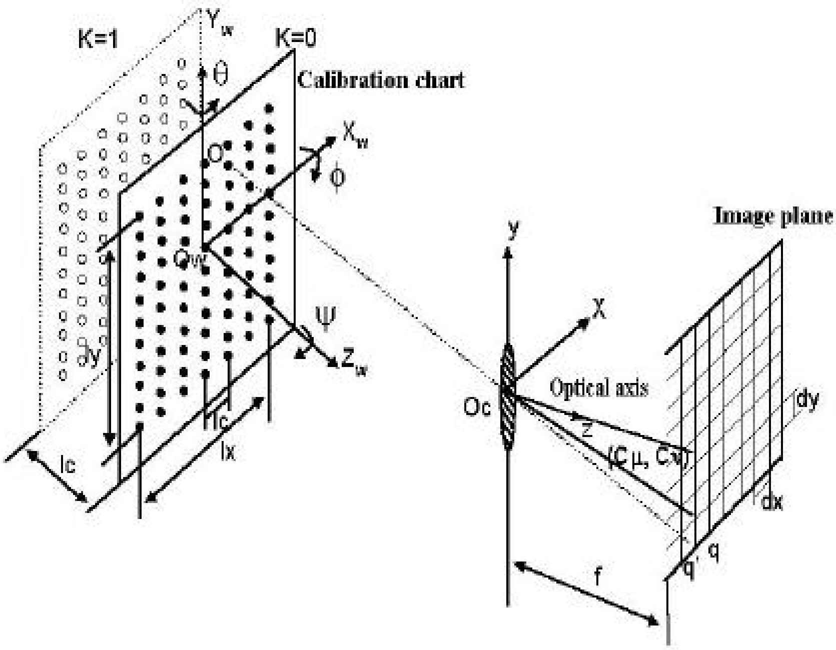

Fig. 3. Setup of calibration chart

The fiducial marks of calibration chart are created by impressing a template of instant lettering graphics sheet containing many black squares on the top surface of acryl block. All the fiducial marks are placed on a plane with uniform interval, lc, in the horizontal and vertical directions. The calibration procedure is to solve the (1) rigid body transform, (2) perspective relation, and (3) radial lens distortion.

$$X_C = RX_W + T \qquad (4)$$

In formula (4), X_C and X_W are the vectors of 3-D camera coordinates and 3-D world coordinates respectively. R is the 3X3 rotation matrix and T is the translation vector. The rotation matrix R can be expressed as function of yaw q , pitch f , and tilt y as follows.

$$R = \begin{bmatrix} \cos y \cos q & \sin y \cos q & -\sin q \\ -\sin y \cos f + \cos y \sin q \cos f & \cos y \cos f + \sin y \sin q \sin f & \cos q \sin f \\ \sin y \sin f + \cos y \sin q \cos f & -\cos y \sin f + \sin y \sin q \cos f & \cos q \cos f \end{bmatrix} \qquad (5)$$

The translation matrix T can be expressed as follows.

$$T = \begin{bmatrix} T_X \\ T_Y \\ T_Z \end{bmatrix} \qquad (6)$$

However, in hazardous environment such as highly radioactivity area, calandria reactor of nuclear power plant, it is impossible to do camera calibration procedure using calibration chart because of restricted access to that area. In this paper, we used a circular pattern of pressure tubes placed on the front face of the calandria with uniform interval, 11.25”(285.75mm), in the horizontal and vertical directions on behalf of calibration chart. The pressure tube layout pattern of the calandria reactor in Wolsung nuclear power plant is shown in Figure 4. The pressure tubes shaped in circular pattern are placed in regular pitch. We can estimate the 3-D world coordinates, X_W, from pressure tube layout pattern placed in regular pitch, 285.75mm, in horizontal and vertical direction. The 3-D camera coordinates, X_C, can be extracted by using the center coordinates of pressure tubes shaped in circular type acquired from image processing sequence. The pressure tube image, shown in Figure 5, for calibration was acquired with a PULNiX TM-7CN CCD camera and a 6X motorized zoom lens, 11.5~69mm, using the setup shown in Fig 10.

The image coordinates, X_C, expressed in crosshairs shown in figure 5, were extracted as follows.

1) Acquire a gray scale image.

2) Threshold the image to produce a binary image. The threshold value was set by analysis of intensity histograms, profiles, and projection method.

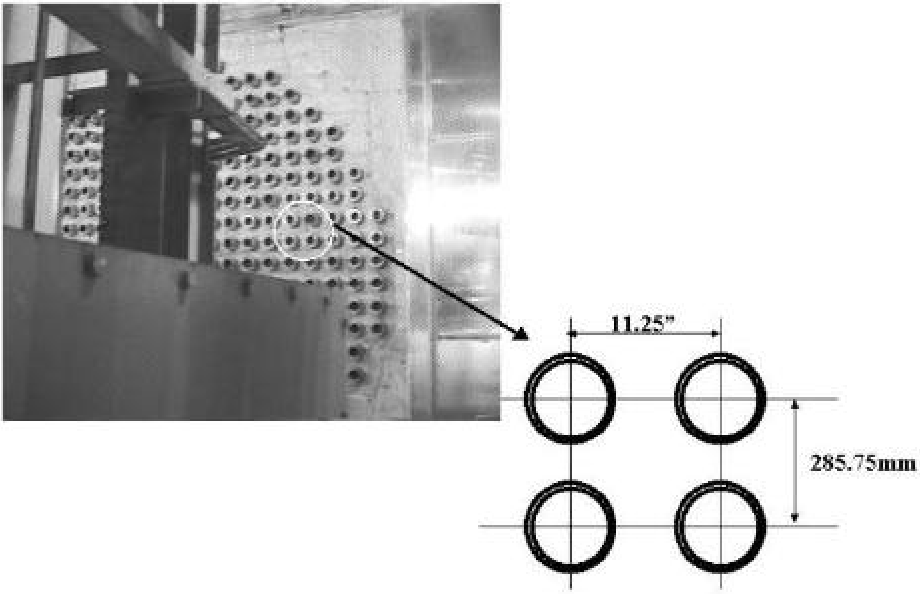

Fig. 4. Pressure tubes of the calandria reactor

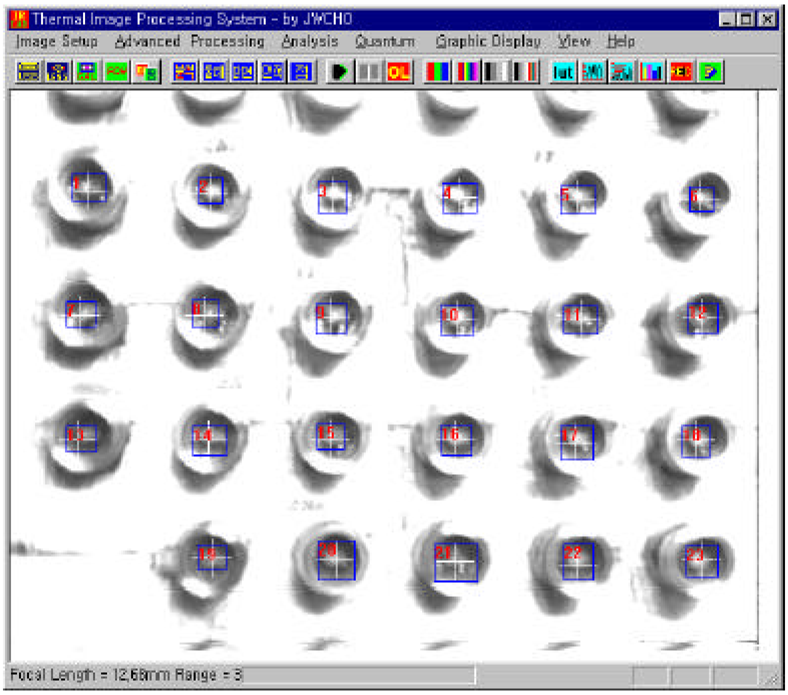

Fig. 5. Pressure tube image of the calandria reactor

3) Segment the individual processing areas, contained single circular pattern only, in the binary image using projection method in vertical and horizontal direction.

4) Calculate the moment of individual tube areas.

5) Fit straight lines to true center points. Then compute intersections, yielding feature point coordinates.

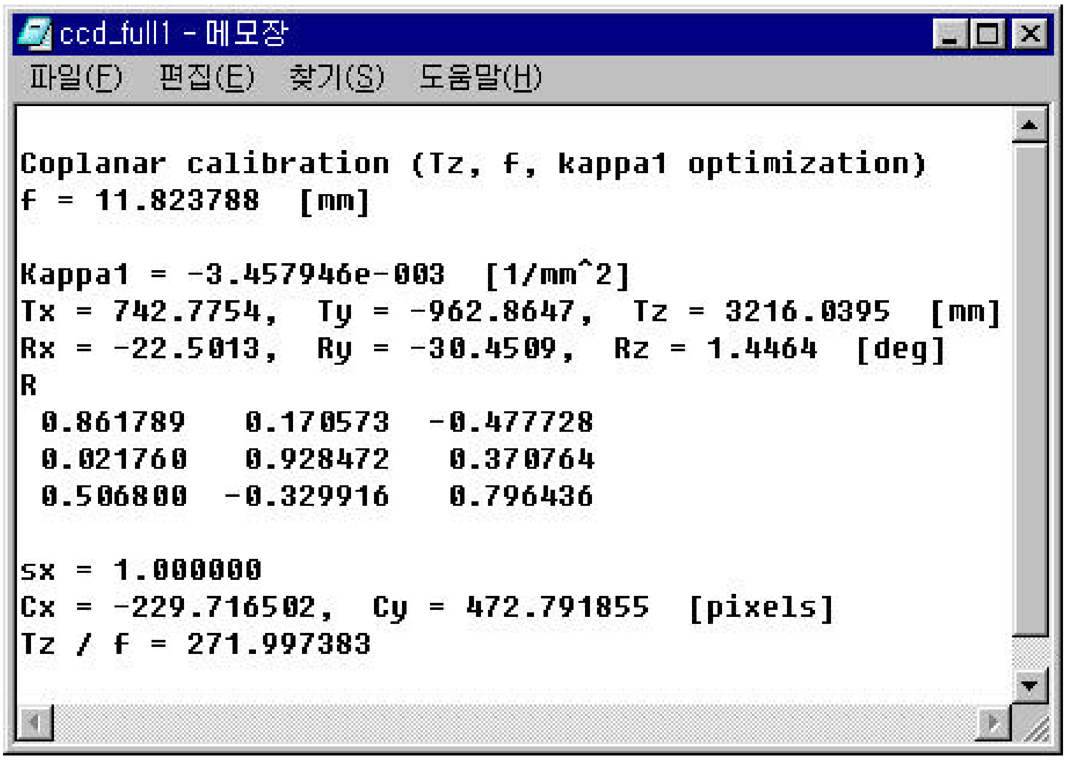

Figure 6. Calibration results of TM-7CN CCD camera

The calibration results of the TM-7CN CCD camera with 6X zoom lens are shown in figure 6.

The C_X and C_Y as shown in figure 6 are image coordinates for the origin in the image plane. A lens distortion coefficient is expressed as k (Kappa1). A S_X is uncertainty scale factor for x, due to CCD camera scanning and acquisition timing error. In the case of zoom lens as shown in figure 6, we could not estimate the focal length of the ones exactly using this calibration method, because two unknown variables, range (T_Z) and focal length(f), are mutually dependent. In order to estimate the focal length more accurately, it is indispensable to get range information. In this paper, we calculated the range using IFOV parameter of THV510 thermal infrared camera expressed in table 1. The 1mrad IFOV parameter of this camera means that the object, 1m in size in the 1km range, is imagined to 1 pixel in the image frame of the thermal camera. This is shown in figure 7. As we know the pitch (285.75mm) shown in figure 4, between the two neighboring pressure tubes, the range from thermal image camera mounted on the mast of mobile robot point to pressure tubes placed on the calandria reactor can be calculated by extracting pixel distance between the center points of neighboring two pressure tubes.

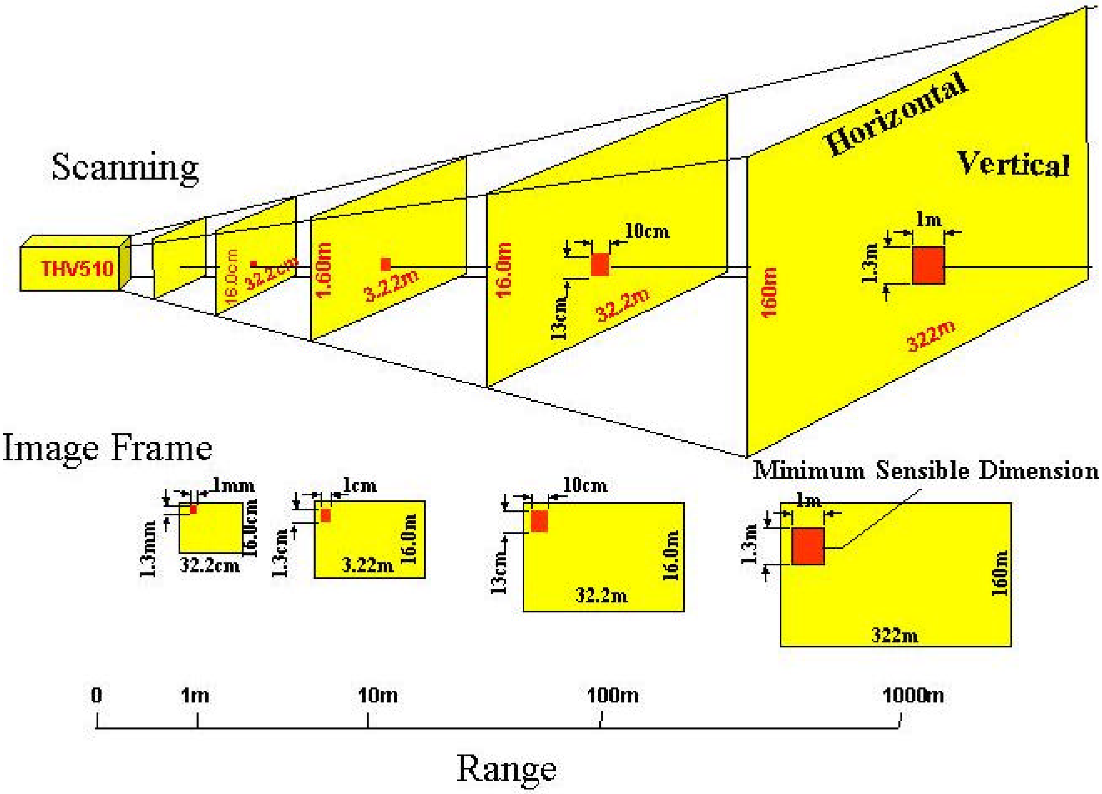

Figure 7. Relationship between distance and scanning range

$$Range = Pitch/\tan q \quad (7)$$

$$q = D_p \cdot IFOV_H \quad (8)$$

Where q is IFOV amount to pitch between neighboring two pressure tubes. In formula (8), D_p is the pixel distance and $IFOV_H$ is instantaneous field of view of THV510 thermal camera in horizontal direction. The pixel distance extraction procedure, shown in figure 8, between these two pressure tubes is nearly the same as the CCD image procedure. The pressure tube thermal image, shown in Figure 9, for range calculation was acquired with a THV510 thermal camera using the setup shown in Fig 10.

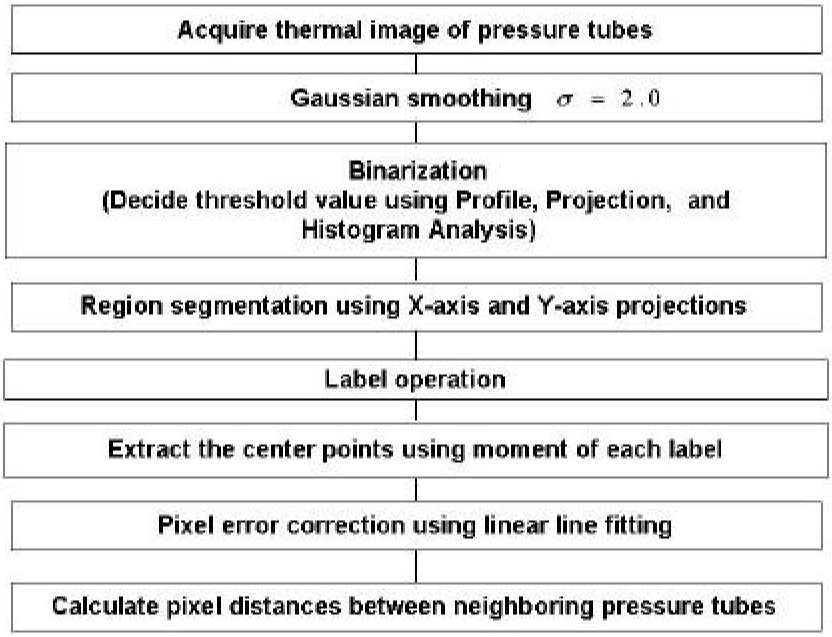

Figure 8. The calculation of pixel distance between neighboring pressure tubes

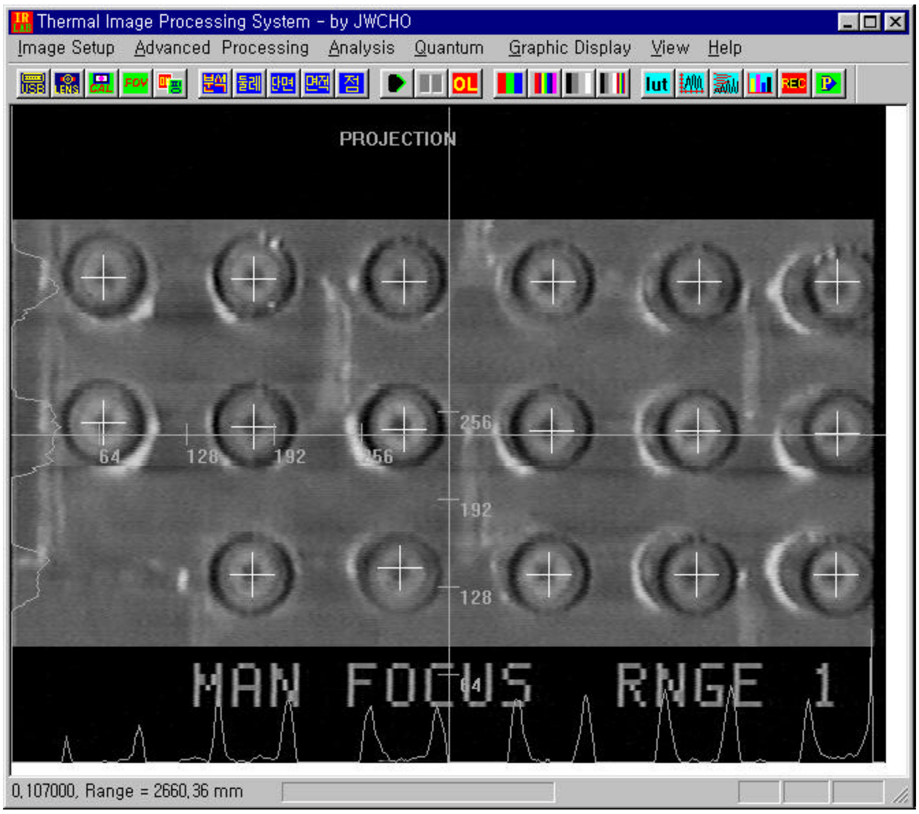

Fig. 9. Thermal infrared image of the pressure tubes

In figure 9, crosshairs represents the center points of the pressure tubes. Using the range found with THV510 thermal image, we could find out the focal length of TM-7CN CCD camera.

4. Experiment and Results

Figure 10 illustrates the KAEROT/m2 mobile robot and control system recently threw into calandria reactor area of Wolsung No.2 nuclear power plant. The inspection head mounted on the mast is designed to move up and down as the positions of nuclear fuel exchange equipment to be monitored. The mobile robot is omni-directionally moved to access the inspection position, via RS-232C interface line, by control command instructed by controller. The controller supplies power needed to drive the mobile robot, mast, pan/tilt unit via 30m cables. The CCD and thermal infrared image, RS-170A video signal, acquired by inspection head mounted on the top of mast are transmitted via RG-59U coaxial cable into the controller for naked-eye inspection and enhanced processing. We developed a CCD/thermal mapping algorithm to superimpose the thermal image into the visible image provided by the THV510, uncooled IR camera, and TM-7CN, CCD camera. We utilize a Matrox Meteor-MC4 frame grabber board, providing for 4-video signal inputs, in an industrial PC rack-mount chassis, with a Pentium host processor card. The software platform is based on Windows 98 operating system and consists of custom native libraries, MIL-LITE 6.1, for image capture, digitizing, memory transfer, and display. Code was written in MSVC6.0 programming language. This is shown in figure 11. The CCD and thermal infrared image from inspection head are stored in VCRs for post analysis and transmitted into frame grabber for online inspection and enhanced processing.

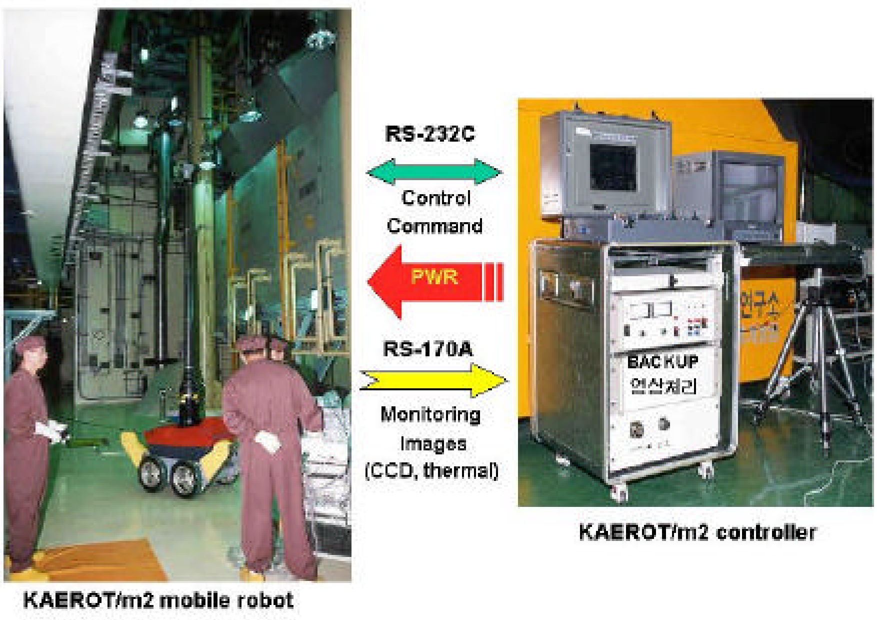

Fig. 10. KAEROT/m2 mobile robot

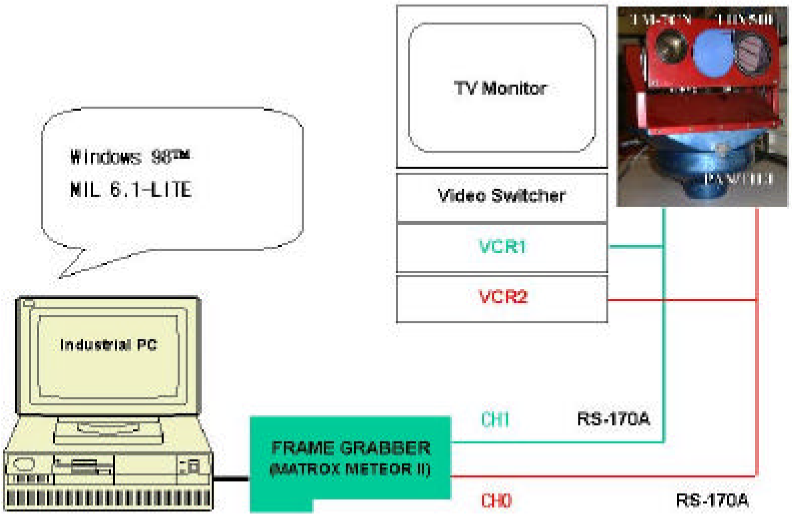

Fig. 11. Hardware and software platform for image processing

We segmented thermal image using threshold method to separate unusual hot image, white areas depicted in figure 9, into background, dark gray image showed in the same one. The segmentation value was set by analysis of intensity profiles. The line-of-sight distance from inspection head mounted on the top of the mast carried by mobile robot to pressure tube is 3229.47mm from the calculation using the thermal image shown in figure 9. And the focal length, 11.87mm, of the TM-7CN is obtained using the ratio T_z / f (271.9973) shown in figure 6, z-axis translation vector (T_z) over focal length (f) and range. Figure 10 illustrates the result by superimposing white areas of thermal image, unusual hot ones, on the gray scale image obtained from TM-7CN CCD camera. The length and diameter of the calandria reactor, which includes 380 pressure tubes, are about 6m and 7.6m, respectively. The inside temperature of the pressure tube is about 300°C. The front of this reactor are sealed with thermal insulation sheets 1m X 1m in size. The unusual hot areas, depicted whitest in the gray level thermal image, of the calandria reactor surface can be seen clearly in the figure 9 and figure 12 bottom-left. These can indicate i) a leakage in pressure tubes, ii) inhomogeneous sealing of the calandria surface, and iii) ambient thermal radiation. The landmark characters, Q R S, for pressure tubes position identification are clearly seen in the CCD image (Figure 12 top-left). By superimposing thermal infrared image into real image we can localize the unusual hot points and areas of calandria reactor surface accurately as shown in figure 12.

(a) 95th frame

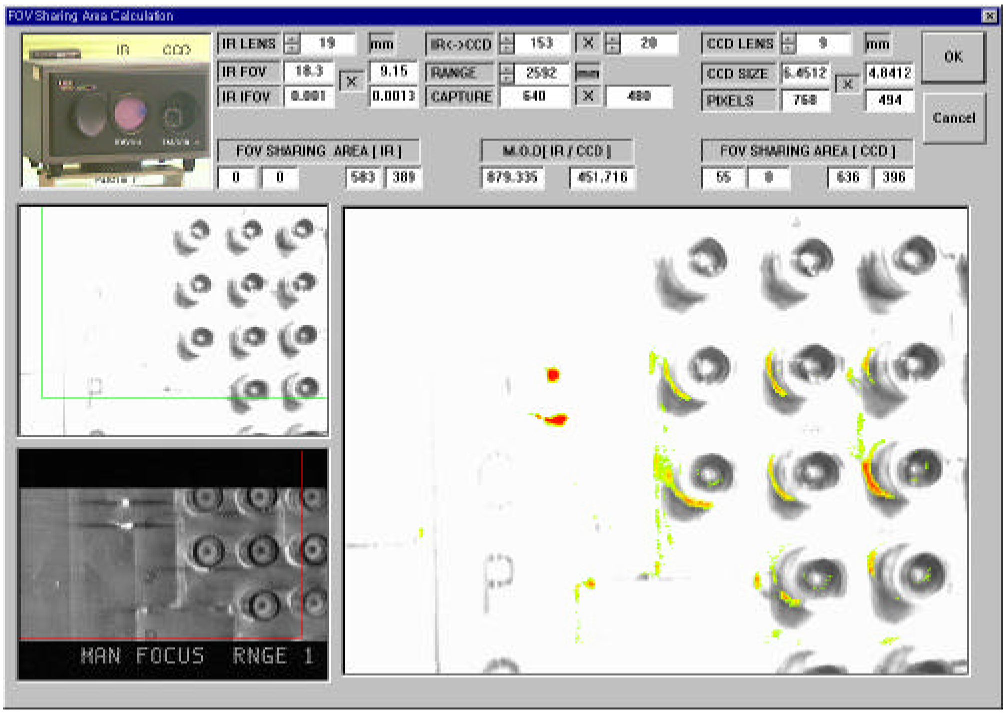

(b) 245th frame

Fig. 12. Superimpose images

5. Conclusions

In this paper an approach to enhance inspection performances for calandria reactor area of Wolsung nuclear power plant through the technique of superimposing thermal infrared image into real CCD image is introduced. In the occurrence of thermal abnormalities on observation points and areas of calandria reactor area, unusual hot image taken from thermal infrared camera is mapped upon real CCD image. We used a circular pattern of pressure tubes placed on the front surface of the calandria reactor as plate for camera calibration needed to match the FOV between thermal camera and CCD camera. The performance of the technique has been evaluated in the experiment carried out at Wolsung nuclear power plant in overhaul period. Localizations of thermal abnormalities on calandria reactor surface can be estimated accurately.

Referenced

[1] J. M. Garner, "IRS – Infrared Research Services vs SSS - The Bottom Line", Proceedings of Thermosense XIV, SPIE Vol. 1682, pp23-29, 1992

[2] N. A. MacNamara and A.E. Hammett, "Development of a Comprehensive IR Inspection Program at a Large Commercial Nuclear Utility", Proceedings of Thermosense XIV, SPIE Vol. 1682, pp30-34, 1992

[3] K.E. Cramer and W.P. Winfree, "Thermographic Detection and Quantitative Characterization of Corrosion by Application of Thermal Line Source", Proceedings of Thermosense XXIV, SPIE Vol. 3361, pp291-300, 1998

[4] R.A. Buchanan, P. Condon, and L. Klynn, "Recent Advances in Digital Thermography for Nondestructive Evaluation", Proceedings of Thermosense XII, SPIE Vol. 1313, pp134-142, 1990

[5] T.S. Jones, E.A. Lindgren, and C.A. Pergantis, "Infrared Inspection of Advanced Army Composites", SPIE Vol. 2473, pp214-218, 1995

[6] Y.W. Qin and N.K. Bao, "Thermographic NDT Techniques for Delaminated Defects in Composite Structures", SPIE Vol. 2473, pp219-223, 1995

[7] N.K. Grande and P.F. Durbin, "Using Emmissivity –corrected Thermal Maps to Locate Deep Structural Defects in Concrete Bridge Decks", SPIE Vol. 2473, pp250-261, 1995

[8] P.F. Durbin, N.K. Del Grande, and P.C. Schaich, "Demonstration of dual-band infrared thermal imaging for bridge inspection. Phase II, final report", UCRL-CR-123341, 1996

[9] S.H. Kim and C.H. Kim, "A Study on Nuclear Power Plant Inspection Tasks using a Mobile Robot", Proceedings of IEEK, Vol. 25. No.1, pp193-196, 2002

[10] Hughes Aircraft, "THV510 Thermovision Maintenance Manual", 1996

[11] R.Y. Tsai, "A Versatile Camera Calibration Technique for High-Accuracy 3D Machine Vision Metrology Using Off-the-Shelf TV Cameras and Lenses" IEEE J. Robotics and Automation, Vol. RA-3, No.4, 323-344, 1987